

Derivative Action Control: Smooth Model Predictive Path Integral Control without Smoothing

Taekyung Kim, Gyuhyun Park, Jihwan Bae, and Wonsuk Lee[†]

Abstract—Here, we present a new approach to generate smooth control sequences in Model Predictive Path Integral control (MPPI) tasks without any additional smoothing algorithms.¹ Our method effectively alleviates the chattering in sampling, while the information theoretic derivation of MPPI remains the same. We demonstrated the proposed method in a challenging autonomous driving task with quantitative evaluation of different algorithms. A neural network vehicle model for estimating system dynamics under varying road friction conditions is also presented.²

I. INTRODUCTION

Controlling an autonomous vehicle in complex environments is a challenging problem. When the vehicle drives on a structured road, it can be modeled as a linear or a kinematic system that is easy to solve. However, the nature of the real world dictates non-linearity and such characteristic is highlighted more at high vehicle speed and low road surface friction. The majority of autonomous driving research has been focused on normal driving conditions, while areas of aggressive maneuvers in highly non-linear environments are yet to be conquered.

Gradient-based trajectory optimization methods have been introduced as powerful solutions for solving the problems of non-linear control systems [1], [2]. However, despite their benefits in solving such problems, such methods still possess the critical flaw that the cost function is not differentiable. This flaw limits the method used to form a quadratic optimization objective, making it ineligible for deployment in real world applications. Sampling-based Model Predictive Control (MPC) has been proposed to optimize both convex and non-convex objectives [3] and has highly benefitted from recent advances in Graphics Processing Units (GPUs). This is because a large number of samples can be computed in parallel to achieve better real-time performance. The major limitation of this approach is that chattering occurs while sampling [4]. Therefore, a smoothing algorithm is required to smooth the control sequence to reduce the damage to the actuators and to improve the system stability. This is true despite the complete irrelevance between optimization theory and this smoothing mechanism. Nonetheless, a conventional smoothing method is not appropriate for MPC because it hinders the controller from achieving optimal control. This

causes many disadvantages while controlling a vehicle near the limits of its performance.

In this paper, we propose a new method to generate smooth control sequences without any additional smoothing algorithms, while preserving the information theoretic interpretation of optimal control theory. Our approach is compared with different smoothing methods in simulated experiments. In addition, we demonstrate our idea using challenging autonomous driving task. An adaptive neural network vehicle model for evaluating the sampled trajectory under varying road friction conditions is also presented.

II. MODEL PREDICTIVE PATH INTEGRAL CONTROL

MPC is a widely studied control theory and there are many successful applications with linear systems. The demand for dynamic and non-linear environmental operations by autonomous robots has been increasing. In several works, ways to handle such issues have been proposed, including sampling-based optimal control [5], [6]. The benefit of the sampling-based method is that it does not require a gradient of the objective function and the cost function. It is not easy for engineers to design a fully differentiable cost function that has a few local minima while encoding the high-level behaviors. In some real-world applications, cost function clipping is inevitable because the system often requires partial state constraints [7]. In contrast to a gradient-based method, a sampling-based method can solve non-convex optimization, in theory. Recent works including MPPI have integrated a sampling-based approach with MPC formulations to mitigate such problems [3], [8]. They combine information theoretic control and stochastic optimal control using free energy and the KL divergence to derive an optimal control distribution with importance sampling [9].

Consider a discrete time dynamic system with a state $\mathbf{x}_t \in \mathbb{R}^n$ and a control input $\mathbf{v}_t \in \mathbb{R}^m$. We applied a general noise assumption that we could not directly control the system over \mathbf{v}_t , but rather over the mean \mathbf{u}_t of the density function of noise ϵ_t :

$$\mathbf{v}_t \sim \mathcal{N}(\mathbf{u}_t, \Sigma).$$

The noise is simply defined as $\mathbf{v}_t = \mathbf{u}_t + \epsilon_t$. Given a sequence of inputs $V \in \{\mathbf{v}_0, \mathbf{v}_1, \dots, \mathbf{v}_{T-1}\}$ and mean input variables $U \in \{\mathbf{u}_0, \mathbf{u}_1, \dots, \mathbf{u}_{T-1}\}$ along a finite time horizon $t \in \{0, 1, \dots, T-1\}$, we can define the probability density function $q(V)$ as:

$$q(V) = \prod_{t=0}^{T-1} Z^{-1} \exp \left(-\frac{1}{2} (\mathbf{v}_t - \mathbf{u}_t)^T \Sigma^{-1} (\mathbf{v}_t - \mathbf{u}_t) \right), \quad (1)$$

The authors are with the Ground Technology Research Institute, Agency for Defense Development, Daejeon 34186, Republic of Korea. {ktk1501, khpark, jihan1008, wsblues}@add.re.kr

[†]Corresponding author

¹<https://github.com/ktk1501/smooth-mppi-pytorch>

²Our video can be found at: <https://youtu.be/o3Nmi0UJFqg>

where $Z = ((2\pi)^m |\Sigma|)^{\frac{1}{2}}$. Similarly, we can also define uncontrolled density function $p(V)$ where U is usually 0:

$$p(V) = \prod_{t=0}^{T-1} Z^{-1} \exp\left(-\frac{1}{2} \mathbf{v}_t^T \Sigma^{-1} \mathbf{v}_t\right). \quad (2)$$

These two density functions correspond to the distribution \mathbb{Q} and \mathbb{P} , respectively. We here define an optimal density function using the free energy of the system [9], which corresponds to the optimal distribution \mathbb{Q}^* :

$$q^*(V) = \frac{1}{\eta} \exp\left(-\frac{1}{\lambda} S(V)\right) p(V), \quad (3)$$

where η denotes the normalizing constant and $S(V)$ denotes the state-dependent cost. The input sequence in state cost is iteratively transformed into state values \mathbf{x} through the system dynamics \mathbf{F} :

$$S(V; \mathbf{F}) = \phi(\mathbf{x}_T) + \sum_{t=0}^{T-1} c(\mathbf{x}_t). \quad (4)$$

As proposed in [4], we can now derive the optimal control input by minimizing the KL divergence between \mathbb{Q} and \mathbb{Q}^* :

$$\mathbb{E}_{\mathbb{Q}^*}[\mathbf{v}_t] = \int q^*(V) \mathbf{v}_t dV. \quad (5)$$

Here, the best solution of (5) is to draw samples directly over \mathbb{Q}^* , but this is not possible. Importance sampling is then employed to compute the integral over the known distribution \mathbb{Q} :

$$\begin{aligned} \mathbb{E}_{\mathbb{Q}^*}[\mathbf{v}_t] &= \int w(V) q(V) \mathbf{v}_t dV \\ &= \mathbb{E}_{\mathbb{Q}_{U, \Sigma}}[w(V) \mathbf{v}_t], \end{aligned} \quad (6)$$

where the importance weighting term is:

$$\begin{aligned} w(V) &= \left(\frac{q^*(V)}{p(V)}\right) \left(\frac{p(V)}{q(V)}\right) \\ &= \frac{1}{\eta} \exp\left(-\frac{1}{\lambda} \left(S(V) + \frac{1}{2} \lambda \sum_{t=0}^{T-1} \mathbf{u}_t^T \Sigma^{-1} (\mathbf{u}_t + 2\epsilon_t)\right)\right). \end{aligned} \quad (7)$$

Let \mathcal{E} be a noise sequence $\{\epsilon_0, \epsilon_1, \dots, \epsilon_{T-1}\}$ and K be the number of trajectory samples. Finally, we have the iterative optimal control update law to compute weights when the sampled trajectory cost $\{C(V^0), C(V^1), \dots, C(V^{K-1})\}$ is given:

$$\mathbf{u}_t^{i+1} = \mathbf{u}_t^i + \sum_{k=0}^{K-1} w(\mathcal{E}^k) \epsilon_t^k \quad (8)$$

$$w(\mathcal{E}^k) = \frac{1}{\eta} \exp\left(-\frac{1}{\lambda} (C(V^k) - \beta)\right), \quad (9)$$

where we subtract the minimum state cost β to ensure that at least one sample has a numerically non-zero importance sampling weight. The trajectory cost in (9) is then simplified as:

$$C(V^k) = S(V^k) + \lambda \sum_{t=0}^{T-1} \mathbf{u}_t^T \Sigma^{-1} \epsilon_t^k. \quad (10)$$

Although the trajectory rollout along the time horizon T must be implemented in a recurrent manner, the perturbed samples K for exploration are parallelizable within the same time step because they are independent from each other [10]. This framework was designed using recent advances of GPUs with CUDA architecture for handling such large parallel samples to achieve real-time performance.

III. PROPOSED DERIVATIVE ACTION CONTROL METHOD

A. Limitations of control smoothing

In Section II, we showed the derivation of an optimal control solution via importance sampling in MPPI. Meanwhile, sampling-based algorithms can impose significant chattering on the control commands when they are applied to the planning and control tasks. A common approach for stability improvement is to smooth the resulting control sequence, *e.g.*, by sliding window smoothing methods or filtering based methods [11]–[13]. It was suggested [4] that a Savitzky-Golay filter (SGF) [14] is an effective solution for such control approaches. It smooths the subsets of adjacent data by fitting the local polynomial approximations in a convolutional manner. However, this kind of smoothing causes negative effects, including system response delay, which stand out when the constraint conditions are given by the actuators. Consider a general state-action system dynamics with clamping function \mathbf{g}_u for handling control constraints:

$$\mathbf{x}_{t+1} = \mathbf{F}(\mathbf{x}_t, \mathbf{g}_u(\mathbf{v}_t)). \quad (11)$$

Since the perturbed control \mathbf{v}_t is bounded by the actuator limits, the sampled noise should be bounded as follows:

$$\bar{\epsilon}_t = \mathbf{g}_u(\mathbf{v}_t) - \mathbf{u}_t. \quad (12)$$

Two possible ways exist to apply SGF in the control sequence.

1) *Smoothing weighted noise sequence*: First, we can apply smoothing to the weighted noise sequence:

$$\mathbf{u}_t^{i+1} = \mathbf{u}_t^i + \text{SGF}\left(\sum_{k=0}^{K-1} w(\mathcal{E}^k) \bar{\epsilon}_t^k\right). \quad (13)$$

It makes data points smoother while compensating the noise that is largely changing along the time horizon. During this procedure, the control variable \mathbf{u} may violate the constraint conditions since the bounded noises are manipulated by the filter. On the other hand, the nature of this process is vulnerable to phase distortion [15], [16]. In addition to violating given constraints, the control sequence will diverge if the noises are overlapped repeatedly and amplified over time. We further describe this phenomenon in Section V-E.

2) *Smoothing control sequence*: Second, we can apply SGF after the control sequence is updated using the weighted noise:

$$\mathbf{u}_t^{i+1} = \text{SGF}\left(\mathbf{u}_t^i + \sum_{k=0}^{K-1} w(\mathcal{E}^k) \bar{\epsilon}_t^k\right). \quad (14)$$

Although this method guarantees that the control variables are meeting the bounded condition, it can cause system

Algorithm 1: Clamping

Given: g_u, g_a : Clamping functions;
 $\mathbf{a}_t, \mathbf{v}_t^k$: Action and derivative action values
 $\bar{\mathbf{a}}_t \leftarrow g_a(\mathbf{a}_t + g_u(\mathbf{v}_t^k)\Delta t)$;
 $\bar{\epsilon}_t^k \leftarrow \frac{\bar{\mathbf{a}}_t - \mathbf{a}_t}{\Delta t} - \mathbf{u}_t$;
return $\bar{\mathbf{a}}_t, \bar{\epsilon}_t^k$

Algorithm 2: SMPPI

Given: \mathbf{F} : Dynamics model;
 K, T : Number of samples, timesteps;
 $(\mathbf{u}_0, \mathbf{u}_1, \dots, \mathbf{u}_{T-1})$: Initial control sequence;
 $(\mathbf{a}_0, \mathbf{a}_1, \dots, \mathbf{a}_{T-1})$: Initial action sequence;
 $\Sigma, \gamma, \phi, c, \Omega$: Control parameters and cost functions;
while task not completed **do**
 $\mathbf{x}_0 \leftarrow \text{SubscribeState}();$
 for $k \leftarrow 0$ **to** $K - 1$ **do**
 $\mathbf{x} \leftarrow \mathbf{x}_0$;
 Sample $\mathcal{E}^k = (\epsilon_0^k \dots \epsilon_{T-1}^k)$, $\epsilon_t^k \in \mathcal{N}(0, \Sigma)$;
 for $t \leftarrow 0$ **to** $T - 1$ **do**
 $\mathbf{v}_t^k = \mathbf{u}_t + \epsilon_t^k$;
 $(\bar{\mathbf{a}}_t, \epsilon_t^k) \leftarrow \text{Clamping}(\mathbf{a}_t, \mathbf{v}_t^k)$;
 $\mathbf{x}_{t+1} \leftarrow \mathbf{F}(\mathbf{x}_t, \bar{\mathbf{a}}_t)$;
 $C_k += c(\mathbf{x}_{t+1}) + \gamma \mathbf{u}_t^T \Sigma^{-1} \epsilon_t^k$;
 $C_k += \phi(\mathbf{x}_T) + \Omega(\bar{\mathbf{a}}_0, \bar{\mathbf{a}}_1, \dots, \bar{\mathbf{a}}_{T-1})$;
 $w_k \leftarrow \text{ComputeWeights}(C_0, C_1, \dots, C_{k-1})$;
 for $t \leftarrow 0$ **to** $T - 1$ **do**
 $\mathbf{U} \leftarrow \mathbf{U} + \left(\sum_{k=0}^{K-1} w_k^T \mathcal{E}^k \right)$;
 $\mathbf{A} \leftarrow \mathbf{A} + \mathbf{U} \Delta t$;
 SendToController(\mathbf{a}_0);
 for $t \leftarrow 1$ **to** $T - 1$ **do**
 $\mathbf{u}_{t-1}, \mathbf{a}_{t-1} \leftarrow \mathbf{u}_t, \mathbf{a}_t$;
 $\mathbf{u}_{T-1}, \mathbf{a}_{T-1} \leftarrow \text{Initialize}(\mathbf{u}_{T-1}, \mathbf{a}_{T-1})$;

response delay. It is common to provide history values since they are required in convolution-based smoothing method. The early values in the control sequence are then affected by the history, which means that the polynomial approximation hinders the controlled distribution from rapidly shifting to an optimal distribution [17]. Note that the first control action is the key value in the MPC problem.

B. Derivative Action Control Method

In this paper, we propose a novel approach called Smooth Model Predictive Path Integral control (SMPPI), to attenuate the chattering in a sampling-based MPC task without extrinsic smoothing algorithms. In the original MPPI, the running control cost in (10) only plays a role in reducing the distance between control values of current and previous iterations [18]. Chattering innately occurs because control trajectory is sampled randomly, and the variance over time in the new control trajectory is not taken into account during optimization. Since applying an additional control cost would violate the theoretical derivation of MPPI, control smoothing

could only be achieved through local fitting algorithms, which bring many disadvantages to the system. Therefore, our framework performs the noisy sampling on a higher order and smooths chattering by the integral operation.

We decouple the control space and action space by defining action sequence $A \in \{\mathbf{a}_0, \mathbf{a}_1, \dots, \mathbf{a}_{T-1}\}$. Substituting (11) into the new system transition model:

$$\begin{pmatrix} \mathbf{x}_{t+1} \\ \mathbf{a}_t \end{pmatrix} = \mathbf{G}(\mathbf{x}_t, \mathbf{v}_t). \quad (15)$$

The control variables now represent derivative actions and they are integrated by time to become action variables:

$$\mathbf{G}(\mathbf{x}_t, \mathbf{v}_t) = \begin{pmatrix} \mathbf{F}(\mathbf{x}_t, \mathbf{a}_t) \\ \mathbf{a}_t + \mathbf{v}_t \Delta t \end{pmatrix}. \quad (16)$$

Additionally, we can apply extra action cost Ω to smooth the action sequence by minimizing the variance of A :

$$\Omega(A) = \sum_{t=1}^{T-1} (\mathbf{a}_t - \mathbf{a}_{t-1})^T \boldsymbol{\omega} (\mathbf{a}_t - \mathbf{a}_{t-1}), \quad (17)$$

where $\boldsymbol{\omega}$ is the weighting parameter in the form of a diagonal matrix. As the control distribution in our proposed method corresponds to derivative action, the action variables can be treated as an augmented state element and become independent from the control cost. Therefore, (17) does not violate the information theoretic interpretation of MPPI. This kind of approach is very effective because our original target for smoothing is action commands, not control sequences.

We then obtain the following action sequence update law:

$$\mathbf{a}_t^{i+1} = \mathbf{a}_t^i + \left(\mathbf{u}_t + \sum_{k=0}^{K-1} w(\mathcal{E}^k) \epsilon_t^k \right) \Delta t, \quad (18)$$

and trajectory cost (10) now takes the form:

$$C(V^k, A) = S(V^k) + \Omega(A + V^k \Delta t) + \lambda \sum_{t=0}^{T-1} \mathbf{u}_t^T \Sigma^{-1} \epsilon_t^k. \quad (19)$$

Finally, we apply two clamping functions of control and action (g_u, g_a) to derive bounded noise $\bar{\epsilon}$ (see Alg. 1). The overall algorithm is shown in Alg. 2.

IV. EXPERIMENTS ON AN INVERTED PENDULUM

We tested MPPI and SMPPI on a simulated inverted pendulum swing up task. It is a simple yet effective benchmark for evaluating control algorithms. The objective of the controller is to hold a pendulum upright by swinging it. The running state cost function $c(\mathbf{x})$ in (4) is formulated as:

$$c(\mathbf{x} \equiv [\theta, \dot{\theta}]^T) = \theta^2 + 0.1\dot{\theta}^2. \quad (20)$$

We designed the neural network dynamics model with two fully-connected hidden layers that each had 32 neurons. The state-action dataset was repeatedly collected during the control procedure and the model was trained with the dataset every 50 time steps. No bootstrap dataset was used since the inverted pendulum system has low enough dimensionality. We compared five different methods: (i) original MPPI

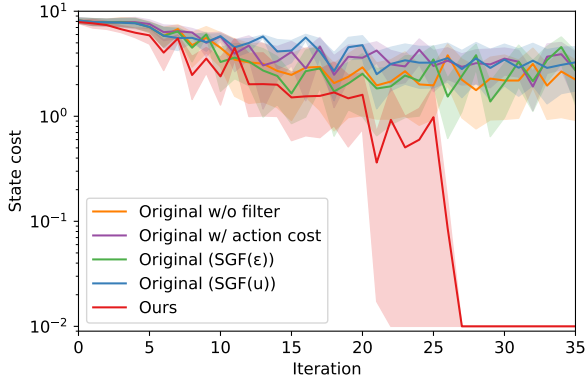


Fig. 1: The average state costs during optimization procedures with different control methods. Each iteration consists of 20 time steps. Note that we apply logarithmic scaling to the y-axis and the costs are clamped to a minimum of 0.01.

without smoothing (8), (ii) applying additional action cost for smoothing on MPPI, (iii) applying SGF on the noise sequence (13), (iv) applying SGF on the control sequence (14), and (v) SMPPI. In this task, control parameters λ and γ were set to 10 and 0.1. For SMPPI, the action sequence cost parameter ω was set to 1. They were tested with seven different initial angular velocities ($\dot{\theta} \in \{-3, -2, \dots, 3\}$), starting from the initial position vertically downward. We fixed the random seed for fair comparison. The state costs (20) during online optimization are shown in Fig. 1. The method (ii) that violates the information theoretic derivation of MPPI had never converged. In contrast, SMPPI was able to quickly make the pendulum upright.

V. EXPERIMENTS ON A VEHICLE SIMULATOR

A. Experiments on a Realistic Vehicle Dynamics Simulator

Our research goal is to perform aggressive driving successfully under challenging conditions, including low friction surfaces and sharp corners. The performance of the model-based control policy is highly dependent on the accuracy of the model [19], [20]. The vehicle model must be trained with all possible maneuvers to minimize model bias. Since the control sequence update is processed by evaluating the perturbed control trajectories with sampling, situations in which control values change significantly over time that make the vehicle unstable should be included in the training dataset. To obtain such data from an actual vehicle would be dangerous. Therefore, we used CarMaker to collect driving data and to evaluate control performances. This is a widely used, high-fidelity vehicle simulator that precisely solves non-linear dynamics in real time.

We built a race track modeled after a real kart circuit named "KART 2000" in Kirchlengern, Germany (see Fig. 2). The length of the track was 1,016 m and it had two moderate curves and four sharp curves. Vehicles should slow down before taking the sharp curves in order not to understeer, which is common on unstructured roads.

B. Low-level Vehicle Speed Controller

In some prior research about autonomous driving on race tracks, electric vehicles were used with no transmissions [4],

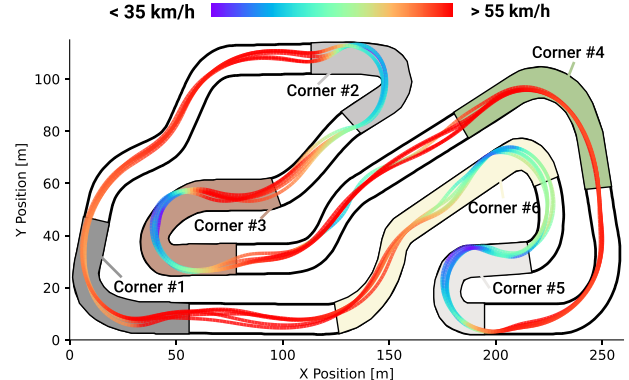


Fig. 2: Trajectory of our proposed method with 60 km/h reference speed.

[21], [22]. Unlike these vehicles, the majority of current vehicles use an automatic transmission to shift gears. The dynamic characteristics of the vehicle are definitely going to change as a gear shifts. Therefore, the throttle control is not adequate to be applied in common vehicles.

In this work, we used speed control with a low-level feedback controller, which manages throttle and brake via a Proportional-Integral (PI) loop. The high-level MPPI controller then takes steering angle (δ) and desired speed (v_{des}) as action variables. A Volvo XC90 was used as the control vehicle.

C. Training Neural Network Vehicle Model

To obtain successfully the open-loop action sequence \mathbf{A} as close as possible to the optimal distribution, precise vehicle dynamics estimation is crucial. We used a feedforward fully-connected neural network with historical information about the state-action pairs. Since the road surface friction is continuously changing while the vehicle drives on unstructured roads, accurate modeling of the non-linear vehicle dynamics is a challenging problem. The vehicle tends to slide on the corners due to low friction and high speed. One solution for this problem is to provide state and action history, which enables the network to capture time-varying behavior at different friction levels [23]. This approach has also been used in other robotics applications, such as helicopters and quadruped legged robots [24], [25]. The overall structure of our vehicle model is shown in Table I. The terms $|\mathbf{x}|$ and $|\mathbf{a}|$ denote the size of the state and action space, and \mathbf{h}_t represents the number of state-action pairs in the previous history. The Rectified Linear Unit (ReLU) is used for activation of hidden layers [26]. The Mean Squared Error (MSE) loss was used as the loss function and Adam optimization was used for the mini-batch gradient descent.

We collected a human-controlled driving dataset in a manner similar to that in our prior work for training a dynamics model [27]. The vehicle state is defined as $\mathbf{x} = [v_x, v_y, r]$, where v_x and v_y are the longitudinal and lateral velocities, and action command is defined as $\mathbf{a} = [\delta, v_{des}]$. We carefully selected three distinct maneuvers:

- i) Zig-zag driving at low speeds (20-25 km/h) on the race track.

TABLE I
OVERALL ARCHITECTURE OF THE VEHICLE MODEL

	Size	Activation
Input	$(\mathbf{x} + \mathbf{a}) \times \mathbf{h}_t$	-
Hidden Layer 1	$2 \times \text{Input Size}$	ReLU
Hidden Layer 2	$4 \times \text{Input Size}$	ReLU
Hidden Layer 3	$6 \times \text{Input Size}$	ReLU
Hidden Layer 4	$2 \times \text{Input Size}$	Linear
Output	$ \mathbf{x} $	-

- ii) High speed driving on the race track, trying to maintain 40 km/h as much as possible.
- iii) Sliding maneuvers in combinations of acceleration and deceleration with small, medium, and large steering angles. Then we controlled the vehicle with rapidly changing commands for random movements, which represent the sampled noisy trajectories of MPPI. They were performed on flat ground in both left and right directions.

Each maneuver was done with multiple road friction coefficients that varied from $[0.4, 0.5, \dots, 1.0]$. The maneuvers on the race track were done in both clockwise and counter-clockwise directions. Each one was logged for two minutes. We collected a total of 35 maneuvers, which amounted to 70 minutes of driving. The dataset were split into two portions: 70% for training and 30% for testing. For evaluating the generalization performance of the trained model, the validation dataset was collected on the modified race track. The default friction coefficient was set to 0.8, and the six corners were assigned with different friction coefficients $[0.95, 0.85, \dots, 0.45]$ that were not included in the driving data for training.

The test and validation errors after training are shown in Table II. The results show that our trained model can precisely represent the vehicle system dynamics regardless of the road friction. The results from estimation of the validation data are shown in Fig. 3. Root Mean Square Error (RMSE) is denoted as \mathbf{E}_{RMS} and the max error is denoted as \mathbf{E}_{max} .

TABLE II
TRAINING RESULTS OF THE NEURAL NETWORK VEHICLE MODEL.

	$v_x \text{ [m/s]}$		$v_y \text{ [m/s]}$		$r \text{ [rad/s]}$	
	\mathbf{E}_{RMS}	\mathbf{E}_{max}	\mathbf{E}_{RMS}	\mathbf{E}_{max}	\mathbf{E}_{RMS}	\mathbf{E}_{max}
Test	0.0311	0.5530	0.0216	0.4723	0.0175	0.2506
Val.	0.0252	0.3744	0.0136	0.1500	0.0123	0.1400

D. Cost Function and Other Parameters

To enable the vehicle to drive inside the given track boundary at high speeds, we designed a state-dependent cost function $c(\mathbf{x})$, which consisted of three components:

$$c(\mathbf{x}) = \alpha_1 \text{Track}(\mathbf{x}) + \alpha_2 \text{Speed}(\mathbf{x}) + \alpha_3 \text{Slip}(\mathbf{x}). \quad (21)$$

The track cost indicates whether the vehicle is inside the track or outside a given boundary. The states of the sampled trajectories are transformed into global positions (p_x, p_y) and they lookup the values of a two-dimensional cost map \mathbf{M} ,

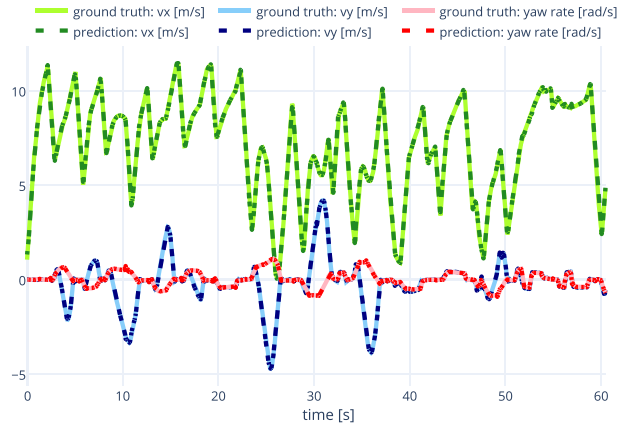


Fig. 3: Estimation results for part of the validation dataset.

which represents the area of outer boundary as 1 and area of inner boundary as 0. Our sampling-based controller allows this impulse-like cost function:

$$\text{Track}(\mathbf{x}) = (0.9)^t 10000 \mathbf{M}(p_x, p_y). \quad (22)$$

The speed cost is the quadratic cost to achieve the reference vehicle speed:

$$\text{Speed}(\mathbf{x}) = (v_x - v_{ref})^2. \quad (23)$$

The slip cost penalizes the sideslip angle to plan a stable future trajectory. Additionally, it imposes a hard cost to reject the samples which are estimated to have a larger sideslip angle than 0.2 radians (approximately 11.46°) in the future:

$$\begin{aligned} \text{Slip}(\mathbf{x}) &= \sigma^2 + 10000 I(|\sigma| > 0.2) \quad (24) \\ \sigma &= -\arctan\left(\frac{v_y}{\|v_x\|}\right), \end{aligned}$$

where I is an indicator function. Since the noise sampling domains of MPPI and SMPPI are different, the variances of the control noise distributions were determined separately. MPPI used $\Sigma = \text{Diag}(4.0, 3.0)$ for the action noise and SMPPI used $\Sigma = \text{Diag}(0.7, 0.4)$ for the derivative action noise. The feedforward control frequency was 10 Hz and the controllers used a time horizon of 4 seconds. The control parameters of K , λ , and γ were 10000, 15.0, and 0.1 during experiments. For SMPPI, it used $\omega = \text{Diag}(0.8, 0.8)$.

E. Experimental Results

We conducted an ablation study for our framework. The track used in these experiments is identical with the one used to collect validation data. We measured average lap times on the six corners during five laps around the track, where the reference speed was set to 40 km/h . If the vehicle went outside a boundary, it was placed at the start point and had to start a new lap. The same pre-trained vehicle model was used and there were no extra training during experiments. The results are shown in Table III.

MPPI with different control update laws (8), (13), (14) failed to complete *Corner 2* and *Corner 3*, which are the sharpest corners of the track. The vehicles collided with the boundary or lost control after taking turns. In contrast, with

TABLE III

AVERAGE LAP TIMES ON THE SIX CORNERS OF DIFFERENT CONTROL METHODS. DETAILED ANALYSIS WAS DONE ON THE MOST SUCCESSFUL METHOD.

Lap time [s]	#1	#2	#3	#4	#5	#6
MPPI w/o Filter	11.08	9.60	N/A	N/A	N/A	N/A
MPPI (SGF(ϵ))	11.75	9.90	N/A	N/A	N/A	N/A
MPPI (SGF(\mathbf{u}))	7.82	N/A	N/A	N/A	N/A	N/A
Ours w/o Ω	8.39	7.71	11.64	8.77	9.86	13.11
Ours w Ω	7.36	7.66	10.83	8.47	9.39	12.86
Min. Speed [km/h]	24.71	20.37	23.30	36.51	28.24	29.77
Max. Slip [degree]	5.34	11.09	9.64	2.91	5.32	4.94

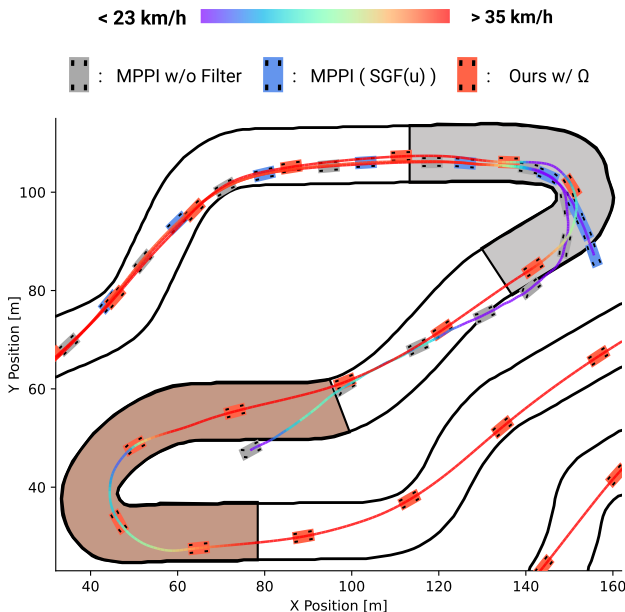


Fig. 4: Visualization of trajectories of the compared controllers. The friction coefficient of corner 2 (in gray) is 0.85 and corner 3 (in brown) is 0.75.

our proposed methods the vehicle traveled the whole lap at high speeds. The trajectories taken by the three controllers are shown in Fig. 4.

On *Corner 2*, the neural network was able to estimate that the vehicle would slide off the track if it did not slow down due to the friction limits. Therefore, it applied the brakes before entering a corner and adjusted the handling angle to make an appropriate turn. During this procedure, the gap between the optimal and the current control sequence increases in an instant. This consequently leads to chattering in the early stage because perturbed samples survive during importance sampling to minimize the impulse-like state cost despite the chattering. In this case, the MPPI controller without smoothing (8) was disturbed by the disadvantage of chattering. This caused the vehicle to take longer to recover its stability. In the case of applying smoothing to the noise (13), repeated phase distortions made the system uncontrollable (see Fig. 5 a). When the smoothing was applied in the control sequence (14) to alleviate phase distortion, the system response slows down since the controller always outputs delayed commands (see Fig. 5 b). The derivative

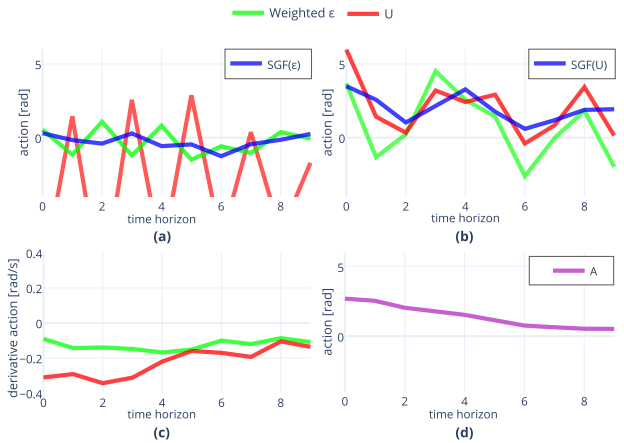


Fig. 5: The first 10 steps of noise, control, and action sequences from different controllers right before entering *Corner 2*. The SGF filter is shown in blue. (a) Control sequence of MPPI (in red) with SGF applied to the noise sequence. (b) MPPI control sequence (in blue) after applying SGF to the original control sequence. (c) SMPPPI control sequence with Ω (in red). (d) SMPPPI action sequence with Ω (in purple).

action sequence of our proposed method still has inevitable chattering, but it is integrated to become a smooth action sequence (see Fig. 5 c-d).

The SMPPPI with action sequence cost Ω shows the best result among the compared methods. This is because reducing the noise in the steer and throttle commands is strongly related to increasing the speed of the vehicle. Our method was also tested with a higher reference speed of 60 km/h. The default friction coefficient was set to 0.9 and those of the corners were set to [1.0, 0.95, ..., 0.75]. It also showed promising results on the challenging roads at varying friction limits (see Fig. 2). We were able to observe the controller taking "out-in-out" trajectories on the sharp corners because this is the best way to preserve high speeds and prevent large slip angles according to the predictions of the neural network model. The average speed during 5 laps was 50.05 km/h and the maximum slip angle was 7.34 degrees.

VI. CONCLUSION

We presented a novel approach to generate smooth control commands in a sampling-based MPC system without any smoothing algorithms. The smoothing effect of the integral shows that it can alleviate the chattering. In addition, our proposed method is not confined to employ action smoothing cost, since the control domain is shifted to the derivative action distribution. We demonstrated that SMPPPI is applicable for a general optimal control task and that it outperforms MPPI with smoothing filters.

We also conducted further experiments of autonomous driving on a challenging race track. We trained our neural network vehicle model with the history of state-action pairs, allowing it to predict accurately the vehicle dynamics, including that of the low-level feedback controller. The SMPPPI was demonstrated to be capable of controlling an autonomous vehicle with agility on sharp and slippery corners. Furthermore, this chattering-free controller is also beneficial in reducing damage to the actuators.

REFERENCES

- [1] W. Li and E. Todorov, "Iterative linear quadratic regulator design for nonlinear biological movement systems," in *ICINCO*. Citeseer, 2004, pp. 222–229.
- [2] Y. Tassa, N. Mansard, and E. Todorov, "Control-limited differential dynamic programming," in *IEEE International Conference on Robotics and Automation (ICRA)*. IEEE, 2014, pp. 1168–1175.
- [3] G. Williams, N. Wagener, B. Goldfain, P. Drews, J. M. Rehg, B. Boots, and E. A. Theodorou, "Information theoretic mpc for model-based reinforcement learning," in *IEEE International Conference on Robotics and Automation (ICRA)*. IEEE, 2017, pp. 1714–1721.
- [4] G. Williams, P. Drews, B. Goldfain, J. M. Rehg, and E. A. Theodorou, "Information-theoretic model predictive control: Theory and applications to autonomous driving," *IEEE Transactions on Robotics*, vol. 34, no. 6, pp. 1603–1622, 2018.
- [5] E. Theodorou, J. Buchli, and S. Schaal, "A generalized path integral control approach to reinforcement learning," *The Journal of Machine Learning Research*, vol. 11, pp. 3137–3181, 2010.
- [6] M. Kobilarov, "Cross-entropy motion planning," *The International Journal of Robotics Research*, vol. 31, no. 7, pp. 855–871, 2012.
- [7] G. Williams, B. Goldfain, P. Drews, K. Saigol, J. M. Rehg, and E. A. Theodorou, "Robust sampling based model predictive control with sparse objective information," in *Robotics: Science and Systems (RSS)*, 2018.
- [8] G. Williams, P. Drews, B. Goldfain, J. M. Rehg, and E. A. Theodorou, "Aggressive driving with model predictive path integral control," in *IEEE International Conference on Robotics and Automation (ICRA)*. IEEE, 2016, pp. 1433–1440.
- [9] E. A. Theodorou and E. Todorov, "Relative entropy and free energy dualities: Connections to path integral and kl control," in *IEEE Annual Conference on Decision and Control (CDC)*. IEEE, 2012, pp. 1466–1473.
- [10] G. Williams, A. Aldrich, and E. A. Theodorou, "Model predictive path integral control: From theory to parallel computation," *Journal of Guidance, Control, and Dynamics*, vol. 40, no. 2, pp. 344–357, 2017.
- [11] S. Särkkä, "Unscented rauch–tung–striebel smoother," *IEEE Transactions on Automatic Control*, vol. 53, no. 3, pp. 845–849, 2008.
- [12] H.-C. Ruiz and H. J. Kappen, "Particle smoothing for hidden diffusion processes: Adaptive path integral smoother," *IEEE Transactions on Signal Processing*, vol. 65, no. 12, pp. 3191–3203, 2017.
- [13] P. Kowalski and R. Smyk, "Review and comparison of smoothing algorithms for one-dimensional data noise reduction," in *International Interdisciplinary PhD Workshop (IIPhDW)*. IEEE, 2018, pp. 277–281.
- [14] A. Savitzky and M. J. Golay, "Smoothing and differentiation of data by simplified least squares procedures," *Analytical chemistry*, vol. 36, no. 8, pp. 1627–1639, 1964.
- [15] S. Tatinati, K. C. Veluvolu, and W. T. Ang, "Multistep prediction of physiological tremor based on machine learning for robotics assisted microsurgery," *IEEE Transactions on Cybernetics*, vol. 45, no. 2, pp. 328–339, 2014.
- [16] K. Adhikari, S. Tatinati, K. C. Veluvolu, and J. A. Chambers, "Physiological tremor filtering without phase distortion for robotic microsurgery," *IEEE Transactions on Automation Science and Engineering*, 2020.
- [17] J. Wang, Y. Ye, X. Pan, X. Gao, and C. Zhuang, "Fractional zero-phase filtering based on the riemann–liouville integral," *Signal Processing*, vol. 98, pp. 150–157, 2014.
- [18] S. Nakatani and H. Date, "Swing up control of inverted pendulum on a cart with collision by monte carlo model predictive control," in *Annual Conference of the Society of Instrument and Control Engineers of Japan (SICE)*. IEEE, 2019, pp. 1050–1055.
- [19] A. Nagabandi, G. Kahn, R. S. Fearing, and S. Levine, "Neural network dynamics for model-based deep reinforcement learning with model-free fine-tuning," in *IEEE International Conference on Robotics and Automation (ICRA)*. IEEE, 2018, pp. 7559–7566.
- [20] R. Sekar, O. Rybkin, K. Daniilidis, P. Abbeel, D. Hafner, and D. Pathak, "Planning to explore via self-supervised world models," in *International Conference on Machine Learning (ICML)*. PMLR, 2020, pp. 8583–8592.
- [21] J. Kabzan, M. I. Valls, V. J. Reijgwart, H. F. Hendrikx, C. Ehmke, M. Prajapat, A. Bühler, N. Gosala, M. Gupta, R. Sivanesan *et al.*, "Amz driverless: The full autonomous racing system," *Journal of Field Robotics*, vol. 37, no. 7, pp. 1267–1294, 2020.
- [22] J. L. Vázquez, M. Brühlmeier, A. Liniger, A. Rupenyan, and J. Lygeros, "Optimization-based hierarchical motion planning for autonomous racing," in *IEEE/RSJ International Conference on Intelligent Robots and Systems (IROS)*. IEEE, 2020, pp. 2397–2403.
- [23] N. A. Spielberg, M. Brown, N. R. Kapania, J. C. Kegelman, and J. C. Gerdes, "Neural network vehicle models for high-performance automated driving," *Science Robotics*, vol. 4, no. 28, 2019.
- [24] A. Punjani and P. Abbeel, "Deep learning helicopter dynamics models," in *IEEE International Conference on Robotics and Automation (ICRA)*. IEEE, 2015, pp. 3223–3230.
- [25] A. Kumar, Z. Fu, D. Pathak, and J. Malik, "RMA: Rapid Motor Adaptation for Legged Robots," in *Robotics: Science and Systems (RSS)*, 2021.
- [26] V. Nair and G. E. Hinton, "Rectified linear units improve restricted boltzmann machines," in *International Conference on Machine Learning (ICML)*, 2010.
- [27] J. Bae, T. Kim, W. Lee, and I. Shim, "Curriculum learning for vehicle lateral stability estimations," *IEEE Access*, vol. 9, pp. 89 249–89 262, 2021.